

LARGE SUPERCONDUCTING DETECTOR MAGNETS WITH ULTRA THIN COILS  
FOR USE IN HIGH ENERGY ACCELERATORS AND STORAGE RINGS\*

M. A. Green

Lawrence Berkeley Laboratory  
University of California  
Berkeley, California

NOTICE  
This report was prepared as an account of work sponsored by the United States Government. Neither the United States nor the United States Energy Research and Development Administration, nor any of their employees, nor any of their contractors, subcontractors, or their employees, makes any warranty, express or implied, or assumes any legal liability or responsibility for the accuracy, completeness or usefulness of any information, apparatus, product or process disclosed, or represents that its use would not infringe privately owned rights.

Abstract

This paper describes the development of a new class of large superconducting solenoid magnets. High energy physics on colliding beam machines sometimes require the use of thin coil solenoid magnets. The development of these magnets has proceeded with the substitution of light materials for heavy materials and by increasing the current density in the coils. The Lawrence Berkeley Laboratory has developed a radical approach to the problem by having the coil operate at very high current densities. This approach and its implications are described in detail.

Introduction

Recent developments in colliding beam physics have prompted the development of thin superconducting solenoid magnets for use in these experiments. The development of thin magnets can be traced starting with PLUTO, the first superconducting magnet which was used to do colliding beam physics. The evolution of thin coil technology can be traced by comparing PLUTO (which is not a thin superconducting magnet) with three other superconducting magnets which have been built or are being built for colliding beam experiments. All three of these magnets are designed to be thin to some degree.

A comparative study of the four magnets illustrates the trend of thin superconducting coil development over the last two or three years. First, one sees the substitution of lighter materials for heavier materials in the CERN magnet. Then one sees the abandonment of cryogenic stability when the bath cryostat is replaced with the tubular cooling system in the CELLO magnet. Finally, the conductive bore tube concept is introduced in order to make a radical improvement in the protection of thin solenoid magnets against burnout. This is the basis of the TPC magnet design proposed by the Lawrence Berkeley Laboratory (LBL).

Over half of this paper will be devoted to the LBL magnet technique. Since the LBL technique is a radical departure from conventional technique, this paper will present the theory of the conductive bore tube and discuss the results of experiments on LBL test coils. Three test coils have been constructed at LBL. Two of these coils, each with a diameter of one meter, have been fully tested and the results are presented herein. Preliminary tests on the third test magnet, which has a diameter of two meters, are described. The results of these tests show the viability of the LBL two-phase tubular cooling system and the conductive bore tube for diverting the magnetic current from the superconducting coil.

The LBL technique is applicable to magnets in a variety of sizes. The radiation thickness attainable is a function of diameter and central induction. This relationship is shown in this paper. In addition, one can apply light superconductors and conductive bore tubes. This can, in principle, result in a reduction of the radiation thickness of solenoids which have a diameter below a certain value.

The development of thin solenoid technology

The development of thin magnet technology can be traced by comparing four colliding beam detector solenoids which have been built or are about to be built. The first of these magnets is PLUTO. This magnet, which makes no effort to be thin, was built in 1971 using the conductor and stabilization technology used in the large bubble chamber<sup>(1)</sup>. The second magnet, ISR, built by Morpurgo at CERN in 1976, substituted a cryogenically stabilized aluminum conductor for the copper conductor normally used<sup>(2)</sup>. The vacuum vessels and cryostat vessels are also made of aluminum. The third step in this progression is the magnet, proposed for the CELLO experiment by Saclay and Karlsruhe, using intrinsically stable aluminum conductor which operates at current densities of  $1.4 \times 10^8 \text{ Am}^{-2}$ <sup>(3)</sup>. The fourth step in the progression is represented by the magnet proposed for the time projection chamber (TPC) experiment by the Lawrence Berkeley Laboratory<sup>(4)</sup>. This magnet uses superconductor at very high matrix current densities (about  $10^9 \text{ Am}^{-2}$ ). The magnet uses a two-phase tubular cooling system.

The four magnets are compared in Table 1. The PLUTO magnet has the largest central induction and smallest free volume. The TPC magnet has both the largest free volume and stored energy. The ISR magnet has the smallest stored energy and it has a central induction of 1.5 T like the CELLO and TPC magnets. The thickest magnet from a radiation standpoint is the PLUTO magnet. The thinnest magnet is the TPC magnet.

\*Work performed under the auspices of U.S. Energy Research and Development Administration.

CP

Table 1. A comparison of four intersection storage ring detector magnets.

	PLUTO (1972)	ISR (1976)	CELLO (1979)	TPC (1980)
Cryostat inner warm diameter (m)	1.40	1.38	1.5	2.0
Distance between the iron poles (m)	1.15	1.80	3.5	3.4
Central induction (T)	2.0	1.5	1.5	1.5
Number of turns	1524	1000	~1400	1950
Current per turn (A)	1264	2200	~3100	2100
Magnet inductance (H)	5.07	1.24	~1.46	4.83
Magnet stored energy (J)	$4.05 \times 10^6$	$3.0 \times 10^6$	$\sim 7.0 \times 10^6$	$10.65 \times 10^6$
Superconductor matrix current density at its design current ( $\text{Am}^{-2}$ )	$4.75 \times 10^7$	$4.07 \times 10^7$	$\sim 1.41 \times 10^8$	$8.75 \times 10^8$
Type of superconductor matrix	Copper	Aluminum	Aluminum	Copper
Radiation thickness (Rad len)	~4.0	~1.10	~0.5	0.38
Cooling system	Bath	Bath	Tube	Tube
Conductive bore tube	No	No	No	Yes
Type of stabilization	Cryogenic	Cryogenic	Adiabatic	Adiabatic
Cold mass (kg)		$\sim 1.7 \times 10^3$	$\sim 1.4 \times 10^3$	$\sim 1.4 \times 10^3$
Type of cryostat vacuum vessel	Stainless Steel	Aluminum	Hexcel	Hexcel

The four magnets shown in Table 1 show the progression of high energy physics toward thinner magnets. It is often desirable to do physics outside the magnet. In order to do this, one must pass large numbers of charged and neutral particles through the magnet over a large solid angle. Therefore, magnets which are thin from a radiation standpoint are used. Before proceeding, it is useful to define radiation thickness. One radiation length will convert about 63% of high energy gamma rays to charged particle pairs. The number of particles  $\Gamma$  which pass through an amount of material unchanged is a function of the original number of particles  $\Gamma_0$  and the radiation thickness  $\lambda$  given in radiation lengths. To the first order this relationship is:

$$\Gamma = \Gamma_0 e^{-\lambda} \quad (1)$$

In general, materials which are thin from a radiation standpoint have low density and low atomic number. The thickness for one radiation length is given in Table 2 for a selection of materials<sup>(3)</sup>.

PLUTO, which is not a thin superconducting magnet, has a radiation thickness which is typical for magnets built with bubble chamber technology<sup>(6)</sup>. In general, the following steps must be taken to reduce a magnet's radiation thickness: (1) Light, low density, low atomic number materials must be substituted for heavier materials. The materials used for cryostat construction are just as important as those used in the magnet itself. (2) The current density of the coil must be increased.

(a) The substitution of low mass materials. The PLUTO magnet, which is shown in Figure 1, is used as a comparison for it is not built with thin coil technology. It uses copper based superconducting coils housed within a stainless steel cryostat. The radiation thickness of PLUTO is estimated to be about four radiation lengths. The ISR magnet built at CERN, which is the first low radiation thickness magnet, employs light materials in both the coil and the cryostat. The superconductor, which is fabricated by soldering a high current density copper-based superconductor to an aluminum stabilizer, is substantially thinner from a radiation standpoint than the PLUTO magnet<sup>(7)</sup>. The ISR magnet cryostat and its vacuum can are fabricated from aluminum. This magnet, shown in Figure 2, is estimated to be about 1.1 radiation lengths thick.

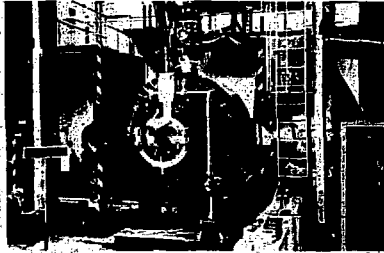


Figure 1. PLUTO superconducting detector magnet at DESY. CBB 778-7379

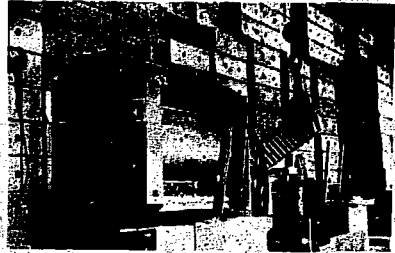


Figure 2. CERN ISR superconducting detector magnet. CBB 778-7381

Table 2. The thickness of various materials which equals one radiation length.

Material	Thickness
Helium (liquid)	7450
Carbon	~ 670
Magnesium	145
Aluminum	90
Copper	14.5
Niobium Titanium (50%Ti)	~ 18
Copper based composite (Cu to s/c ratio, 1-2)	16.1-15.5
Aluminum based composite (Al to s/c ratio, 1-2.5)	30-42
Epoxy-dacron	~ 360
Epoxy-glass	~ 180

The proposed CELLO and TPC magnets go a step further toward lighter construction. Both use a tubular cooling system, discussed in the next section, which will reduce the helium vessel thickness. The outer vacuum vessels proposed for the CELLO and TPC magnets involve the use of composite or hexcel type materials. Large cryogenic vacuum vessels must resist buckling due to pressure forces. Hexcel, which is a honeycomb structure, will provide the thickness needed to resist buckling without adding material. As a result, the expected cryostat vacuum vessel thickness for these magnets is expected to total 0.06-0.1 radiation lengths. The use of light vacuum vessel material is especially important for magnets as they grow in size. The TPC magnet which has an outside diameter of about 2.3 m will have a hexcel outer vacuum vessel 30-40 mm thick. The proposed TPC experiment is shown in Figure 3. The TPC magnet cross section is shown in Figure 4.

(b) Increasing superconductor matrix current density. The second step for reducing magnet thickness is to increase the current density within the superconducting coil. Both PLUTO and the ISR magnets operate at low current densities which are typical of those found in cryogenically stabilized magnets. Figure 5 shows the current density in the superconductor matrix as a function of stored magnetic energy for a number of superconducting magnets which have been built. The magnets are divided into two broad categories—those which use adiabatic stability (most of these magnets have stored energies under  $10^6$  J and current densities above  $10^8$  Am<sup>-2</sup>) and those which use cryogenic stability (these magnets have stored energies above  $10^6$  J and current densities below  $6 \times 10^7$  Am<sup>-2</sup>). From Figure 5 one can see that the ISR magnet does not make a departure from the norm. If anything, the design is very conservative.

The CELLO magnet proposal calls for operating at matrix current densities which are 3 to 3.5 times larger than PLUTO or the ISR magnet. This conductor is operated at current densities which are, in general, too high for cryogenic stability. The coil is operated as an adiabatically stable coil; hence it can quench. Quenching can damage the coil unless the coil and its quench protection circuit are properly designed. The  $J_0^2 B_0 = 10^{23}$  line represents a

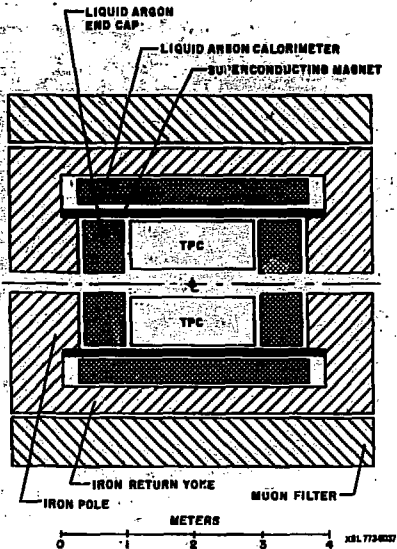


Figure 3. Cross section of the experiment showing the location and size of the superconducting magnet.

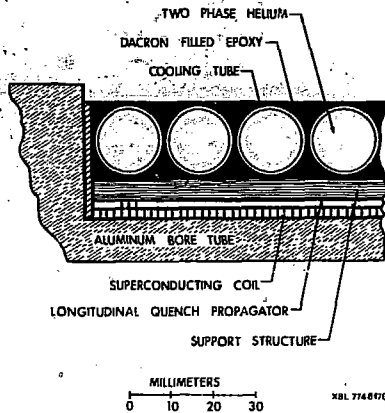


Figure 4. Cross section of the proposed TPC solenoid coil.

practical limit for the design of magnets without an inductively coupled bore tube<sup>(8)</sup>. The CELLO magnet lies a little above that line. It can do so because its current is over 3000 A and the coil can withstand voltages during a quench in excess of 1000 V.

The TPC magnet and the Lawrence Berkeley Laboratory test coils leading up to it (see Fig. 5) represent a radical departure from normal practice. These magnets are designed to operate at superconductor current densities which are in excess of  $8 \times 10^8 \text{ Am}^{-2}$ . At this

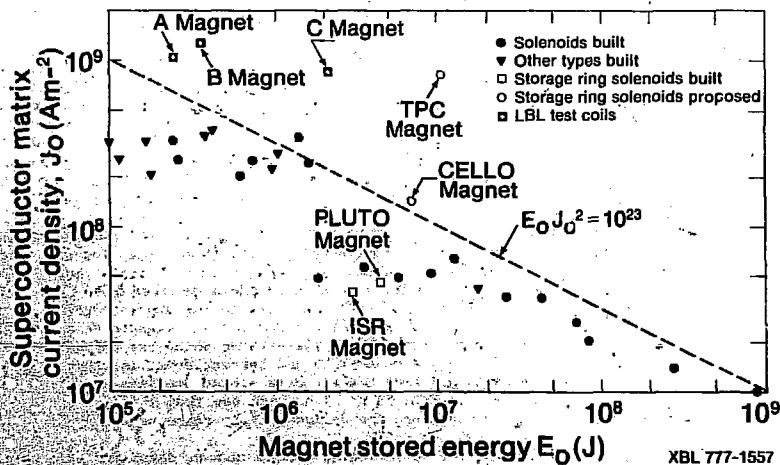


Figure 5. Superconductor matrix current density vs. magnetic stored energy for a number of magnets which have been built or are proposed.

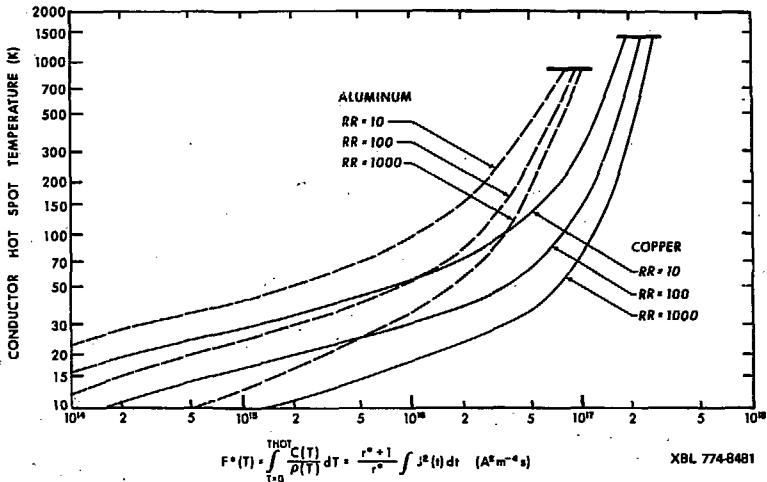


Figure 6. Superconductor hot spot temperature versus  $F^*(T)$ .

current density, destruction during a quench can occur very quickly. The TPC magnet has  $J_0^2 E_0 \approx 8 \times 10^4$ . Such operation using normal magnet construction methods would require high current operation (say  $10^4$  A) and high quench protection voltages (say  $10^4$  V). Instead, the TPC magnet relies on a closely coupled bore tube for quench protection. As a result, the TPC magnet has the highest stored energy and lowest radiation thickness of any of the four magnets.

**Development of the TPC magnet concept.** Since the proposed TPC magnet is a radical departure from normal magnet construction technique, it is useful to discuss its development. There are two primary features in the TPC magnet which set it apart from the others: (1) The magnet has an inductively coupled bore tube for quench protection. (2) The magnet is cooled by two-phase helium flowing in tubes. The TPC magnet integrates the cryostat (the helium temperature part) and the coil into one construction. The basic design for the TPC magnet emerged in early 1975, when a smaller detector magnet was being proposed. The bore tube technique has been refined and experimental tests have taken place. The results of these tests are presented in the next section.

(a) **The closely coupled conductive bore tube technique.** Large thin solenoids are potentially subject to destruction during a quench. Coil failure is either due to (1) hot spot formation due to uneven quench energy distribution in the coil, or (2) excessive transient voltages needed to overcome hot spot development. Sometimes both will occur at the same time. The upper boundary of hot spot temperature can be found by assuming that a small section of the superconductor is heated by resistive heating and that there is no heat transfer out of that section. This approximation is valid once that small section of superconductor has reached 30K or above. The hot spot temperature can be found from the following integral expression:

$$F^*(T) = \int_0^T \frac{C(T)}{\rho(T)} dT = \frac{1+r}{r} \int_0^{\infty} j(t)^2 dt \quad (2)$$

where  $C$  is the specific heat per unit volume of the superconducting matrix;  $\rho$  is the electrical resistivity of the normal metal in the matrix;  $r$  is the normal metal to superconductor ratio in the conductor;  $j$  is the current density in the superconductor matrix;  $T$  is temperature; and  $t$  is time.

Figure 6 relates  $T$  to  $F^*(T)$ , hence to the integral  $j^2 dt$ . It is clear from this figure that one must reduce the conductor current density as quickly as possible to reduce the hot spot temperature. It is also clear that one must reduce the current density even faster when an aluminum based superconductor is used. At current densities of  $10^9$  Am<sup>-2</sup>, the current in the magnet must be reduced substantially in times of the order of 100 ms. In large magnets, this cannot be done without large transient voltages unless a closely coupled low resistance bore tube is used or the whole coil is driven normal at once.

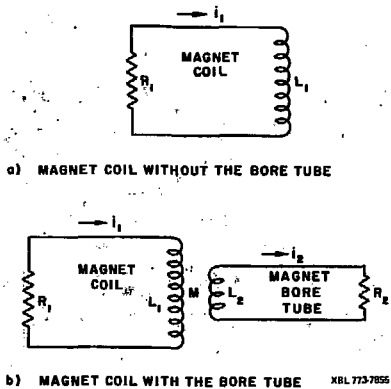


Figure 7. Electrical circuit diagram for a magnet with and without a conductive bore tube.

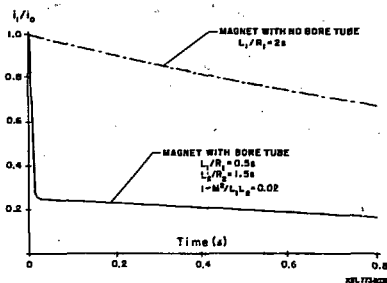


Figure 8. Current in the magnet versus time for a magnet with and without a bore tube.

Figure 7 shows the circuit diagrams for quenching magnets with and without a bore tube. The decay of the magnet current  $i_1$  in the magnet without the conductive bore tube is represented by

$$L \frac{di_1}{dt} + i_1 R_1 = 0 \quad (3)$$

where  $i_1 = i_0$  (the starting current) at  $t = 0$ . The solution for Equation 3 takes the form:

$$i_1 = i_0 e^{-t/\tau_1} \quad (4)$$

when  $L_1$ , the magnet inductance, and  $R_1$ , the magnet circuit resistance, are constant.  $\tau_1$  (the circuit time constant) =  $L_1/R_1$ .

The decay of the current in the magnet  $i_1$  takes a different form when a closely coupled bore tube is introduced. The differential equations for this case are:

$$L_1 \frac{di_1}{dt} + M \frac{di_2}{dt} + i_1 R_1 = 0, \quad (5)$$

$$L_2 \frac{di_2}{dt} + M \frac{di_1}{dt} + i_2 R_2 = 0$$

where  $i_1 = i_0$  and  $i_2 = 0$  when  $t = 0$ .  $L_2$  is the bore tube inductance;  $R_2$  is the bore tube resistance; and  $M$  is the mutual inductance between the coil and the bore tube. If the coil and bore tube are closely coupled,  $\epsilon = 1 - M^2/L_1L_2 \ll 1$ . If one assumes  $\epsilon$  small (say  $< 0.05$ ) and  $L_1$ ,  $L_2$ ,  $M$ ,  $R_1$  and  $R_2$  are constant, then the solution to  $i_1$  in Equation 5 becomes

$$i_1 = \frac{i_0}{(\tau_L - \tau_S)} (\tau_1 - \tau_S) e^{-t/\tau_L} + (\tau_L - \tau_1) e^{-t/\tau_S} \quad (6)$$

where  $\tau_S$  is the short time constant and  $\tau_L$  is the long time constant. When  $\epsilon$  is small,  $\tau_S$  and  $\tau_L$  take the following forms:

$$\tau_L = \tau_1 + \tau_2, \quad (7a)$$

$$\tau_B = \frac{\epsilon \tau_1 \tau_2}{\tau_1 + \tau_2} \quad (7b)$$

where  $\tau_2$  (the bore tube time constant) =  $L_2/R_2$ .

When  $\tau_2$  is large compared to  $\tau_1$ , the current in the coil takes a sudden dip to a fraction of its starting value. Then the current decays slowly (see Figure 8). The sudden dip in the coil current  $i$  is accompanied by a sudden rise in the bore tube current  $i_2$ . The total flux contained in the magnet changes very slowly with the time constant  $\tau_1$ . As a result, the transient voltages are kept within reasonable bounds. The shift in current away from the coil reduces the integral of  $j^2 dt$  without large transient voltages<sup>(9)</sup>. The bore tube absorbs a portion of the magnetic energy in the process. The unexpected bonus is that the bore causes the whole coil to go normal much faster than ordinary quench propagation. This phenomenon, which is referred to as "quench back," has a positive effect on fail safe operation of large high current density coils.

(b) The tubular cooling system. The cryogenic system of all large superconducting magnets presents a number of major problems. The two-phase tubular cooling system solves most of these problems<sup>(10)</sup>. One is not restricted to pool boiling heat transfer in a bath of helium once one decides to use an adiabatically stable superconductor. Liquid helium flowing in tubes will provide all of the cooling needed for a dc solenoid magnet. The advantages of a tubular cooling system over an ordinary bath cooled system are: (1) the cooldown of the magnet is well controlled because the helium flows in a well-defined path, (2) the mass of a tubular cooling system is less than a bath cryostat (so is the radiation thickness), (3) helium in direct contact with the coil is minimized, and (4) the cryogenic safety is greatly enhanced because tubes have very high pressure ratings and the ratio of helium volume to free vacuum is minimized.

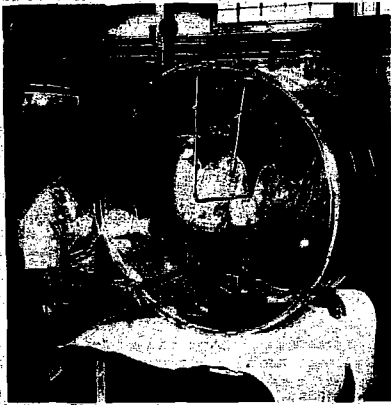
The LBL system uses two-phase helium instead of the supercritical helium which is used in OMEGA or the SIN magnet. Two-phase helium was chosen because (1) a two-phase boiling system will operate at lower temperatures than a comparable single-phase system, (2) the temperature varies very little from end to end in a two-phase system, (3) the mass flow for a given amount of refrigeration is lower for the two-phase system than for a supercritical system, and (4) boiling in the tube can transfer large local heat fluxes. The stability of the two-phase flow is achieved by choosing the right flow regime. The liquid and gas should travel at the same velocity. When the mist or bubble and froth flow is chosen, the fluid is well behaved like a single-phase flow.

The Lawrence Berkeley Laboratory experiments. LBL has built two-meter diameter solenoids which have been operating for nearly two years. The latest LBL test coil, which was finished in June of 1977, has a diameter of two meters, a length of 0.7 meters, and a stored energy which is 2.0 MJ (one-fifth that of the TPC magnet). The one-meter diameter magnets have been tested extensively. The two-meter test magnet tests have only begun.

(a) The one-meter test solenoids. The LBL one-meter diameter solenoids are approximately 0.5 meter long with just over 830 turns of 1.1 mm diameter (including insulation) superconductor wound on them<sup>(11)</sup>. The primary difference between the two coils is the copper to superconductor ratio of the superconductor. The A magnet uses an MCA superconductor with 2200 12.3- $\mu$ m filaments twisted one turn every 10 mm and with a copper to superconductor ratio of 1.8. The B magnet uses a Supercon superconductor with 2700 13.6- $\mu$ m filaments twisted one turn every 10 mm. Its copper to superconductor ratio is 1.0. Both coils are wound on an 1100-0 aluminum bore tube 6.35 mm thick. On top of the coil is a layer of 12.7 mm OD aluminum tube for cooling. Both coils are vacuum impregnated with epoxy. There are many small differences between the two magnets. The B magnet is much better than the A magnet. For example, the epoxy in the A magnet has cracked, causing the coil to move away from the bore tube as magnetic force is applied. The B magnet shows no evidence of cracking and, hence, we have not encountered training. Figure 9 shows one of the 1-meter diameter magnets. Figure 10 shows a cross-section of the magnet bore tube, coil and cooling tube.

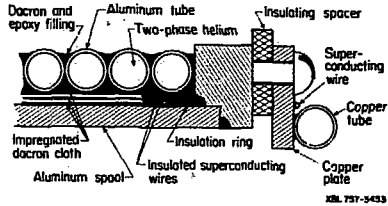
A number of the tests of the A and B magnets have been described in other reports<sup>(12-15)</sup>. Most of the discussion here will be centered upon the tests of new kinds of quench protection circuits and tests of the A and B magnets hooked in series. Before proceeding, it is useful to point out that the bore tube behaves as theory suggests it would. Figure 11 illustrates the shift in current from the coil to the bore tube. It shows a sudden drop in coil starting at a time of 50 ms which ends at a time of 100 ms. This sudden drop in the coil current, balanced by sudden rises in the bore tube current, is caused by quenchback. It is also useful to point out that the tubular cooling system has performed very well through a half-dozen tests of the A and B coil. Detailed operating data of the cooling system is found in reference 15.

The use of a conductive bore tube enhances the performance of quench protection systems. LBL tested three kinds of quench protection systems: (1) a constant resistance resistor of



CBB 762-2054

Figure 9. The LBL one-meter diameter solenoid (coil B).



XBL 757-3453

Figure 10. The LBL one-meter diameter solenoid coil cross section.

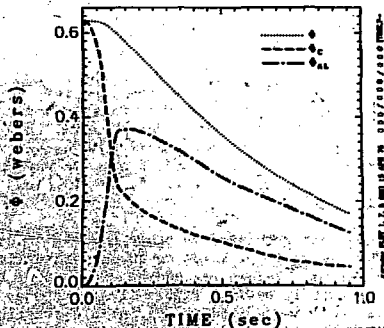
0.6 ohms, (2) a variable tyrite resistor called a variator, and (3) the discharge of a capacitor bank into the coil to drive it normal. The A magnet, B magnet and A & B magnets can be quenched in a fail-safe manner without the use of an external quench protection circuit. The use of such circuits will reduce the integral of  $j^2 dt$ , hence the hot spot temperature.

Figure 12 shows current versus time at 400 A in the B magnet for an unprotected quench, a protected quench with a 0.6 ohm resistor put across the leads and a protected quench with a variator across the leads. One can see quenchback in the unprotected quench. It takes over 100 ms for quenchback to start. When quenchback is finished, the current decays exponentially from about 30 percent of its former value. The hot spot temperature reaches 300 K and 60 to 70 percent of the coil energy ends up in the bore tube.

When a 0.6 ohm resistor is put across the leads (this occurs some 10 ms after the quench is induced), the current in the coil is reduced to 50 or 60 percent of its starting value immediately. Quenchback takes place dropping the coil current to 25 percent of its starting value. The resistor reduced the hot spot temperature to around 90 K while forcing over 80 percent of the magnet energy into the bore tube. The effectiveness of the resistor is greatly enhanced by the bore tube.

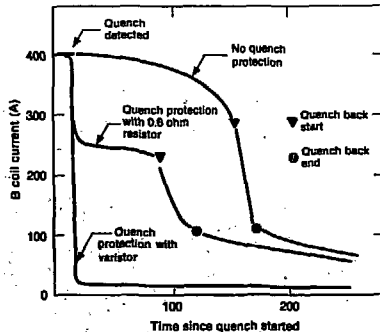
AA01. TEST 6. LOG 2. RUN 47.

$I_0 = 700$ ,  $U_0 = 18$



XBL 758-8844

Figure 11. Magnetic flux due to currents in the coil  $\phi_c$ , bore tube  $\phi_b$  and both current  $\phi_{AL}$  versus time for the 700 A quench in the A coil.



XBL 777-1064

Figure 12. B coil current versus time for various quench protection systems.



The varistor system is characterized by a resistance which takes the following form:

$$R = R_0 \left( \frac{i}{i_0} \right)^{b-1} \quad (8)$$

where  $b$  is 0.2 to 0.25. When  $i = 400$  A,  $R \approx 3.6$  ohms. The varistor causes the coil current to suddenly drop to only a few percent of its starting value in less than 5 ms ( $\tau_0$ , the short time constant, is 2 - 3 ms). The integral  $\int i^2 dt$  is dominated by what happened before the quench was detected. In any event, when the hot spot temperature drops below 40 K, the bore tube ends up with virtually all of the magnet stored energy. The conductive bore tube greatly enhances the performance of the varistor system. Without the conductive bore tube, the varistor system would only be marginally better than a constant resistor of value  $R_0$ .

The third method of quench protection is by driving the coil entirely normal through the use of a capacitor bank. The A and B magnets have a high frequency inductance of around 10 mH. If a capacitor bank is discharged into the coil in a short time, the coil will see a sudden surge of current (of short time duration) which will drive the entire coil normal (by momentarily pushing the current in the superconductor above its critical current). Once the entire coil is normal, current is shifted to the bore tube and the coil hot spot temperature is greatly reduced. A short pulse of a couple of hundred volts drove the B magnet normal very well during recent tests of the A and B magnets together. Neither the varistor nor this method of quench protection would be effective without the conductive, closely coupled bore tube.

Table 3 summarizes the operating characteristics of the A magnet, the B magnet and the A and B magnet together in series. The B magnet has never trained even though it has operated at current densities of  $1.24 \times 10^9$  Am<sup>-2</sup>. Training due to coil movement has occurred in the A magnet when it has operated alone or in conjunction with the B magnet. The magnets were quenched without protection at all of the peak currents given in Table 3. The tests have demonstrated full safe operation (without quench protection) substantially above the  $j_0 E = 10^{23}$  line shown in Figure 5.

Testing of the A and B solenoids was completed in June 1977. The magnets have been shipped to the Sandia Laboratory in Albuquerque, New Mexico, USA, in order to become part of a pulsed MHD generator<sup>(16)</sup>. The magnets have demonstrated they can handle considerable abuse. For example, an electrical lead was burned out due to inadequate gas flow. The magnet was driven normal without damage by the overheated electrical lead. The lead became hot enough to melt some solder joints causing leaks into the cryogenic vacuum system. The A and B magnet tests showed the inherent safety of the closely coupled bore tube system and the two-phase tubular cooling system.

Table 3. The operating characteristics of the A magnet, B magnet and A + B magnets in series.

	A Magnet	B Magnet	A + B Magnet
Design current (A)	700	800	700
Critical current (at 4.8 K) (A)	910	1150	830
Number of turns	835	832	1667
Length (m)	0.461	0.464	1.0
Magnet diameter (ID) (m)	1.021	1.021	1.021
Design matrix current density Am <sup>-1</sup>	$0.909 \times 10^9$	$1.120 \times 10^9$	$0.909 \times 10^9$
Self inductance (H)	0.789	0.782	1.949
Design stored energy (J)	$1.931 \times 10^5$	$3.028 \times 10^5$	$4.775 \times 10^5$
Peak operating current (A)	804*	972**	704*
Peak matrix current density (Am <sup>-2</sup> )	$1.044 \times 10^9$	$1.238 \times 10^9$	$0.914 \times 10^9$
Peak stored energy (J)	$2.547 \times 10^5$	$3.694 \times 10^5$	$4.830 \times 10^5$

\* The magnet trained; this is the highest current the magnet trained to.

\*\* No magnet training to this current. This current was the limit of the power supply.

(b) The two-meter diameter test coils. A two-meter diameter test coil was wound and potted during Spring of 1977. The magnet has an inside diameter of 1980 mm; its length is 765 mm, and its thickness is 36 mm. The radiation thickness of the magnet is approximately 0.36 radiation lengths. The two-meter test magnet, called the C magnet, has about 5500 m of 1.5-mm diameter superconductor which has 2200 19.6- $\mu$ m diameter filaments. The copper superconductor ratio in the conductor is 1.8 and it has a twist pitch of 20 mm. The C magnet tubular cooling system consists of 365 m of 12.7-mm OD aluminum tubing.

The construction of the C magnet is similar to the A and B magnets. The bore tube is made from 9.53 mm thick 1100-0 aluminum plate; 860 turns of superconductor are wound in 20 layers on to the bore tube (see Fig. 13). Between the layers is a center tap. A quench propagator system is wound on top of the upper layer of superconductor. This winding is bifilar; it proceeds longitudinally (lengthwise) down the coil in 12 places around the coil to speed up the turn-to-turn quench velocity. (The A and B coils do not have longitudinal quench propagators.) Above the quench propagators are two layers of 3.18-mm diameter aluminum wire which serves as a support to prevent the coil from lifting away from its bore tube. The aluminum cooling tube was wound on the outside, then the magnet was vacuum impregnated. The total mass of the finished magnet including its four leads and the bar assembly is 420 kg. The finished magnet is shown in Figure 14.

After epoxy casting, the coil was high-potted to 8.2 kV to ground. The magnet was put into a 2.4-m diameter nitrogen shielded vacuum vessel which is 1.2-m high. Instrumentation on the coil included 8 strain gages with 6 dummy gages, 12 quench coils, 2 coils for measuring  $d\phi/dt$ , 4 voltage taps (one for each electrical lead), 7 silicon diode thermometers, 2 vapor bulb thermometers, 7 strain gage thermometers, and 2 pressure taps in the cryogenic circuit. The instrumentation was connected to various oscilloscopes and to a PDP-11 computer which acted as a data collector and preprocessor. Data from the PDP-11 is processed by the LBL 7600 computer.

Testing was started on the C coil in July 1977. At the time this paper was written, only one series of tests had been completed. The first test of the magnet was terminated by an accident which broke the magnet supports and damaged the plumbing. The magnet survived; it quenched as would be expected after moving several centimeters before colliding with the vacuum vessel. The accident was caused by iron in the capacitor bank which was being used to protect the magnet from quenching. The accident occurred at a current of 957, which is just over half the magnet's critical current. At the time the magnet contained 890 kJ of magnetic energy and it was operating at a coil current density of  $5.4 \times 10^8$  Am<sup>-2</sup>. The accident showed us, unintentionally of course, that integrated magnet design is extremely rugged. Quenches at low currents showed that positive quench protection could be achieved.

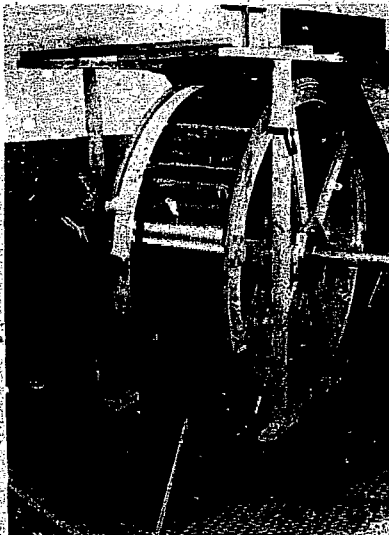


Figure 13. Winding of the two-meter diameter test solenoid.

CBB 773-1666

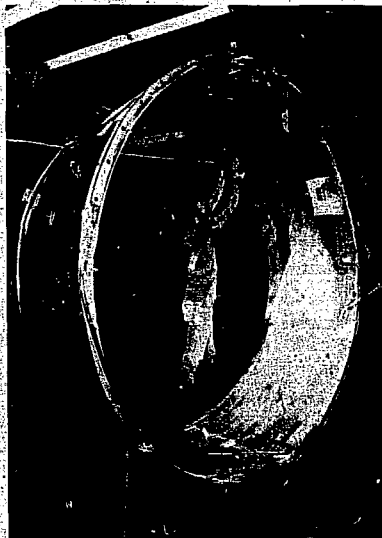


Figure 14. The completed LBL two-meter diameter test solenoid.

CBB 776-6029

Table 4. The characteristics of the LBL two-meter diameter test magnet.

	Single Layer*	Double Layer
Average coil length (m)	0.6968	0.6968
Average coil diameter (m)	2.0062	2.0043
Number of turns	430	860
Magnet coil inductance (H)	0.462	1.847
Bore tube inductance (H)	$2.39 \times 10^{-6}$	$2.39 \times 10^{-6}$
Mutual inductance between coil and bore tube (H)	$9.87 \times 10^{-4}$	$1.973 \times 10^{-3}$
Design current (A)	2000	1500
Superconductor current density at design current ( $\text{Am}^{-2}$ )	$1.131 \times 10^9$	$0.849 \times 10^9$
Magnet stored energy at design stored current (J)	$0.924 \times 10^6$	$2.078 \times 10^6$

\*The outer layer which is near the quench propagator.

We saw evidence that the magnet quench circuits were working as intended. The expected performance of the C magnet is shown in Table 4.

The future course of thin magnet technology. The Lawrence Berkeley Laboratory thin coil development program has been rather conservative. We have not devoted a great deal of effort toward the use of a suitable high current density aluminum based superconductor. The use of aluminum based superconductor could reduce the radiation thickness of the superconductor nearly in half. Paper studies have been made of coil systems which use aluminum based superconductors wound on magnesium bore tubes with a magnesium cooling tube system. With this kind of technology, one could, in theory, reduce the radiation thickness of the TPC solenoid from 0.38 radiation lengths to 0.26 radiation lengths. However the risk of using untested technology is not justified.

High current density aluminum based superconductors are light. They have roughly half the radiation thickness of copper based conductors. The quench wave velocity is about a factor of three faster in the aluminum based conductor than in a copper based conductor operating at the same current density. If aluminum based superconductors are used in conjunction with an aluminum bore tube, the structure will be particularly good from a thermal contraction and relative strain standpoint. The major disadvantage of the aluminum based superconductor is the fact that  $F^*(T)$  and hence the integral of  $j^2 dt$  is a factor of 3 to 5 smaller than for a

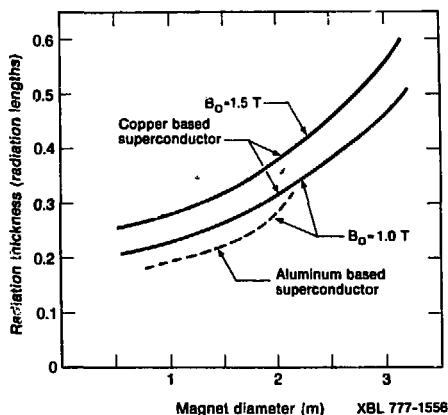


Figure 15. The projected radiation thickness of thin solenoids using the LBL technique as a function of magnet diameter, superconductor type and central induction  $B_0$ .

copper based superconductor. Particular care must be taken to avoid burn-out problems associated with the use of this type of conductor.

Figure 15 shows the total radiation thickness including the cryostat as a function of diameter for magnets with central inductions of 1.0 and 1.5 tesla. The two upper curves apply for magnets using copper based superconductors. The lower curve, which is a 1 tesla central induction curve, applies when aluminum based superconductor is used. The use of a conductive bore tube should permit one to operate magnets when  $E_{0j_0}^2$  is as high as  $10^{25}$ . (By comparison, magnets without conductive bore tubes and limited to operation below  $E_{0j_0}^2 = 10^{23}$ . For coils made with aluminum stabilized conductor,  $E_{0j_0} < 0.4 \times 10^{23}$ ).

#### Acknowledgments

This work would not have been possible without the dedicated efforts of many people on the LBL staff. Thanks go to P. H. Eberhard, M. A. Garajost, G. Gilson, R. Ross, R. Smit, J. D. Taylor, V. Vuillemin and other people in the Physics division. Particular thanks must go to P. B. Miller and the LBL mechanical shops for the skill and effort which went into the construction of the test solenoids.

#### References

1. W. Eschricht et al. "The Operation of a Three-Coil 5 Megajoule Superconducting Magnet System at the Electron Positron Storage Ring DORIS," a DESY report, Hamburg, W. Germany, 1976.
2. M. Morpurgo, "Design and Construction of a Superconducting Aluminum Stabilized Solenoid," Cryogenics, p. 89, February 1977.
3. "Proposal for a 4 $\pi$  Magnetic Detector for PETRA (CELLO)," a proposal by DESY, IEKP Karlsruhe, MPI Munchen, Orsay, Paris University and Saclay, August 1976.
4. "A Proposal for a PEP Facility Based on the Time Projection Chamber," PEP-4, December 1976.
5. "Particle Properties," April 1974, taken from review of Particle Properties, Physics Letters 50B (1), p. 74, 1974.
6. C. P. Parsch et al, "The 1.4m/2.2 Tesla Superconducting Detector Magnet PLUTO for the Electron Positron Storage Ring at DESY," Proceedings of the 4th International Conference on Magnet Technology, 1972.
7. M. Morpurgo and G. Pozzo, "Fabrication of an Aluminum Stabilized Superconductor," Cryogenics, p. 87, February 1977.
8. P. H. Eberhard et al, "Quenches in Large Superconducting Magnets," Lawrence Berkeley Laboratory, LBL 6718, August 1977, and these proceedings.
9. P. H. Eberhard, M. A. Green, R. G. Smits and V. Vuillemin, "Quench Protection for Superconducting Solenoids with a Conductive Bore Tube," Lawrence Berkeley Laboratory, LBL-6444, May 1977.
10. M. A. Green, "The Large Superconducting Solenoid for the Minimag Experiment," Advances in Cryogenic Engineering 21, p. 24, 1975, and Lawrence Berkeley Laboratory, LBL 3677, July 1975.
11. M. A. Green and J. D. Taylor, "Construction of the A Coil," Lawrence Berkeley Laboratory internal report UCID 3835, March 1976.
12. M. A. Green, P. H. Eberhard and J. D. Taylor, "Large High Current Density Superconducting Solenoids for Use in High Energy Physics Experiments," in Proceedings of the 5th International Cryogenic Engineering Conference, Grenoble, France, May 11-14, 1976; also, Lawrence Berkeley Laboratory, LBL 4824.
13. P. H. Eberhard, M. A. Green, W. B. Michael, J. D. Taylor and W. A. Wenzel, "Tests on Large Diameter Superconducting Solenoids Designed for Colliding Beam Accelerators, IEEE Transaction on Magnetics," MAG-13(1), 78, January 1977, and Lawrence Berkeley Laboratory LBL 5364, Aug. 1976.
14. M. A. Green, "Large Diameter Thin Superconducting Solenoid Magnets," Cryogenics, p. 17, January 1977; also, Lawrence Berkeley Laboratory LBL-5515.
15. M. A. Green, "The Development of Large High Current Density Superconducting Solenoid Magnets for Use in High Energy Physics Experiments," Doctoral dissertation, University of California at Berkeley, Lawrence Berkeley Laboratory, LBL-5350, May 1977.
16. M. Cowan et al, "Pulsed Energy Conversion with a D.C. Superconducting Magnet," Cryogenics p. 699, December 1976.